Nuclear Engineering and Technology xxx (xxxx) xxx

Contents lists available at ScienceDirect

Nuclear Engineering and Technology

journal homepage: www.elsevier.com/locate/net

Original Article

Impact of boundary layer simulation on predicting radioactive pollutant dispersion: A case study for HANARO research reactor using the WRF-MMIF-CALPUFF modeling system☆

Kyo-Sun Sunny Lim [a], Jong-Myung Lim [b], Jiwoo Lee [c, *], Hyeyum Hailey Shin [d]

[a] School of Earth System Sciences, Kyungpook National University, 80, Daehak-ro, Buk-gu, Daegu, 41566, South Korea
[b] Environmental Radioactivity Assessment Team, Korea Atomic Energy Research Institute, 111, Daedeok-daero 989, Yuseong-gu, Daejeon, 305-353, South Korea
[c] Lawrence Livermore National Laboratory, P.O. Box 808, Livermore, CA, 94551, USA
[d] National Center for Atmospheric Research, P.O. Box 3000, Boulder, CO, 80307-3000, USA

ARTICLE INFO

Article history:
Received 4 November 2019
Received in revised form
26 May 2020
Accepted 8 June 2020
Available online xxx

Keywords:
CALPUFF
Dispersion of radioactive material
WRF
Wind fields
Stability calculation

ABSTRACT

Wind plays an important role in cases of unexpected radioactive pollutant dispersion, deciding distribution and concentration of the leaked substance. The accurate prediction of wind has been challenging in numerical weather prediction models, especially near the surface because of the complex interaction between turbulent flow and topographic effect. In this study, we investigated the characteristics of atmospheric dispersion of radioactive material (i.e. ^{137}Cs) according to the simulated boundary layer around the HANARO research nuclear reactor in Korea using the Weather Research and Forecasting (WRF)-Mesoscale Model Interface (MMIF)-California Puff (CALPUFF) model system. We examined the impacts of orographic drag on wind field, stability calculation methods, and planetary boundary layer parameterizations on the dispersion of radioactive material under a radioactive leaking scenario. We found that inclusion of the orographic drag effect in the WRF model improved the wind prediction most significantly over the complex terrain area, leading the model system to estimate the radioactive concentration near the reactor more conservatively. We also emphasized the importance of the stability calculation method and employing the skillful boundary layer parameterization to ensure more accurate low atmospheric conditions, in order to simulate more feasible spatial distribution of the radioactive dispersion in leaking scenarios.

1. Introduction

Wind is one of the most important meteorological factors in the case of unexpected radioactive pollutant dispersions, determining the distribution and concentration of the leaked substances [1,2]. Stronger winds under more unstable atmospheric conditions transport the radioactive pollutant farther away from the source, while weaker winds in a more stable stratified atmosphere keep the radioactive pollutant near the source. Accurate prediction of wind is therefore one of the key factors in forecasting radioactive dispersion.

The wind prediction has been conducted using numerical weather prediction (NWP) models, which are advanced and large-scale versions of computational fluid dynamics (CFD) models that solve the Navier-Stokes equation via the finite difference method. The NWP models solve not only the dynamic equations but also the thermophysical equations to simulate various meteorological phenomena. Among them, accurate simulation of wind has been one of the major challenges, especially at the near surface atmospheric level, due to the confounding factors of friction with the uneven surface of the Earth and the complex turbulence in the atmospheric boundary layer. In NWP models, a special component called the planetary boundary layer (PBL) parameterization controls the calculation of vertical distribution of the near-surface wind field. The PBL scheme determines vertical wind profiles according to the roughness of the surface and the turbulence characteristics of the PBL.

☆ May 2020 under review at ***Nuclear Engineering and Technology*** *(SCI-E, IF 1.546)*.

* Corresponding author.
E-mail address: jwlee@llnl.gov (J. Lee).

https://doi.org/10.1016/j.net.2020.06.011

The Korea Atomic Energy Research Institute (KAERI) has set up a dispersion prediction system based on a combination of the Weather Research and Forecasting (WRF) model, and the California puff (CALPUFF) atmospheric transportation model [3,4]. The WRF Model is a community-developed open-source NWP model [5] that has been widely used in the field of atmospheric science to conduct operational weather predictions [6], meso-scale meteorology research [7–9], climate simulations [10–13], and dispersion predictions and studies [3]. The CALPUFF model is a multi-layer, non-steady-state gridded puff dispersion model capable of simulating the impacts of spatial and temporal variations in meteorological conditions upon the transport, wet and dry deposition, and chemical transformation of pollutant species [14,15]. The detailed method for the treatment of diffusion processes in the CALPUFF model is described in the user guide [14].

In the WRF model, various PBL parameterization schemes have been implemented up to date [5]; however, no consensus has been made for the best performing scheme for every case. Not surprisingly, because different regions have different meteorological and geological characteristics, the performances of PBL schemes vary depending on the region of interest. One of PBL schemes that has been widely applied is Yonsei University (YSU) PBL scheme [16,17]. It computes the vertical profiles of meteorological parameters (e.g., winds, temperature and moisture) considering influence from small-scale turbulences near the surface. One of the main features of the scheme is its explicit representation of the turbulent entrainment processes at the top of the PBL, which bring relatively warm and dry air into the PBL from the free atmosphere above [16,18]. The good performance of the YSU PBL has been demonstrated for the Korean and East Asian regions by its application in many meteorological and climatological studies e.g., [7,8,19–21].

In the present study, the dispersion characteristics of radioactive materials (^{137}Cs) are examined in the KAERI's WRF-Mesoscale Model Interface (MMIF)-CALPUFF system with the purpose of advancing the dispersion predictability. In particular, the impacts of the following components upon the near-surface wind are examined: (1) orographic drag consideration in the WRF, (2) stability calculation in the MMIF coupler, and (3) selection among different PBL parameterizations in the WRF. The KAERI's High-flux Advanced Neutron Application Reactor (HANARO), a 30 MW multi-purpose research nuclear reactor located at Daejeon, Republic of Korea, was selected for a hypothetical radioactive leaking scenario. The methodology and experimental set-up are described in Section 2. The results of the simulation experiments are described in Section 3, and the summary and conclusions are in the final section.

2. Methodology

2.1. Model and data

The meteorological fields are generated using the WRF model version 3.6 [22]. It is a fully compressible non-hydrostatic model with the Arakawa-C grid system. Table 1 summarizes the physics parameterizations, which are identical to those used in our previous study [4]. The model's physics package includes the WRF Single-Moment 6-class microphysics scheme (WSM6) [23] with the new mixed-phase hydrometeor fall speeds [24], the Kain–Fritsch (KF) scheme for cumulus parameterization [25,26], the Unified Noah Land Surface Model [27], the Rapid Radiative Transfer Model for general circulation models (RRTM-G) longwave and shortwave radiation schemes [28,29], and the YSU PBL scheme [16,17] along with the revised surface-layer orographic drag scheme [30]. The cumulus parameterization was only applied to the outermost domain, 1 [4].

The WRF model configuration consists of three layers of nested domains defined on Lambert conformal projection (Fig. 1). The 1-km innermost grid model centered at Daejeon (Domain 3) is surrounded by the 3-km grid model (Domain 2). The outermost grid has a 9-km resolution covering the Korean Peninsula. The outer domains provide boundary conditions for their inner domains via the one-way interaction nesting approach. High-resolution 3-s topography data from the Shuttle Radar Topography Mission (SRTM) [31,32] and land-cover data (http://egis.me.go.kr), are used for the high-resolution simulation using the WRF model. The model is set to have 40 vertical layers with the lowest model level height where wind fields are predicted is approximately at 25 m (i.e., the bottom layer depth is approximately 50 m).

Following the procedure described in Lim et al. (2019) [4], 102-h integration was performed starting at 00 UTC on each day during October 2016. The month of October is climatologically characterized by low wind speed, compared to other months [4]. The reason why we choose October 2016 is to figure out the impact of sub-grid orographic parameterization on simulated wind field during the period experiencing low wind speed. The initial conditions (ICs) and boundary conditions (BCs) were obtained every 6 h from the 12-km horizontal-resolution Regional Data Assimilation Prediction System (RDAPS) operated in the Korea Meteorological Administration (KMA). The analysis fields from the RDAPS were applied during the first 24 h of simulation (00, 06, 12, and 18 UTC) for the ICs and BCs in the KAERI model system and the forecast fields of the RDAPS were applied for BCs in the rest 78 h of the simulations, in order to generate the higher-resolution (9-, 3-, and 1-km) meteorological fields using the WRF model. This set-up enables the operation of a real-time forecasting system.

The MMIF version 3.3, the interface framework between WRF and CALPUFF, takes the meteorological fields, including topographic height and land-use, generated by the WRF model and generated input parameters such as stability and PBL height for the CALPUFF dispersion model. The choice of the PBL scheme in WRF can affect the simulated wind field, PBL height, turbulence field. The interval time of the WRF model output is set to 1 h, which is the same for the interval time of ingested CALPUFF input. The model domain for the CALPUFF is the same as the innermost domain of the WRF model shown in Fig. 1 but excluding five grid points at the border areas of the model domain. The levels of the vertical grids are set to 0, 20, 40, 80, 160, 320, 640, 1,200, 2,000, 3,000, and

Table 1
Summary of the physics parameterizations.

Physics parameterization	Employed scheme	Reference
Planetary boundary layer	Yonsei University planetary boundary layer (YSU PBL) scheme	Hong et al. (2006)
Shortwave/Longwave radiation	Rapid Radiative Transfer Model for General Circulation Models	Iacono et al. (2008) Morcrette et al. (2008)
Land surface model	Unified Noah land surface model	Chen and Dudhia (2001)
Cloud microphysics	WRF single-moment 6-class (WSM6) microphysics scheme	Hong and Lim (2006)
Cumulus	Kain–Fritsch (Turned off for Do 2 and 3)	Kain (2004) Kain and Fritsch (1990)

Please cite this article as: K.-S. Sunny Lim et al., Impact of boundary layer simulation on predicting radioactive pollutant dispersion: A case study for HANARO research reactor using the WRF-MMIF-CALPUFF modeling system, Nuclear Engineering and Technology, https://doi.org/10.1016/j.net.2020.06.011

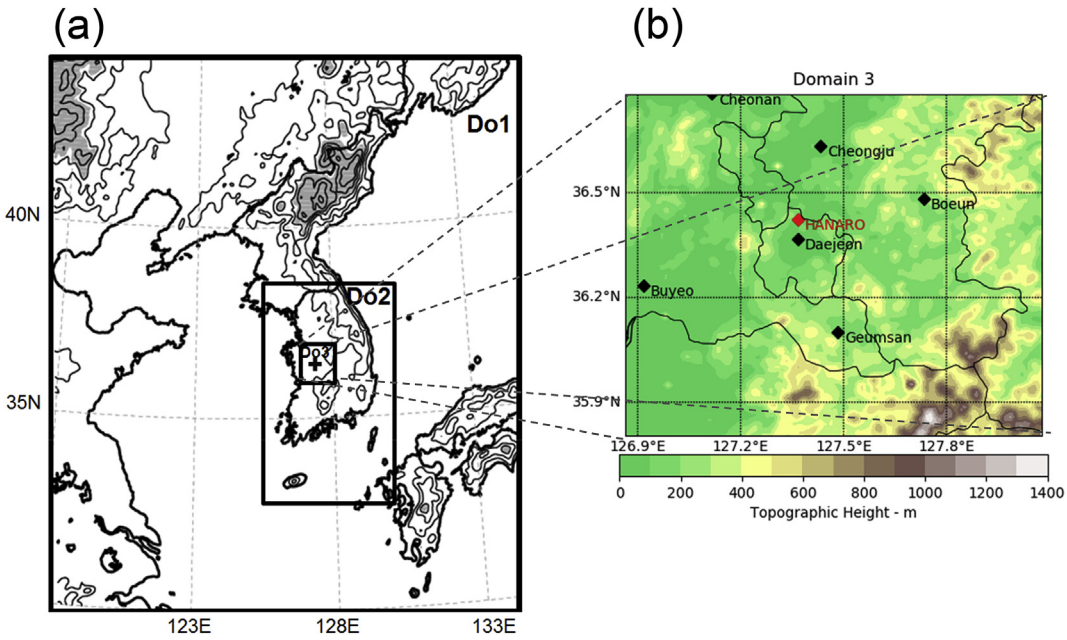

Fig. 1. (a) Model domain configuration for meteorological model of WRF with terrain contoured every 300 m for the 9-km resolution grid (Do1). The resolutions of the inner domains (Do2 and Do3) are 3 and 1 km. Terrain height values greater than 1000 m are shaded in gray. (b) Model domain for the CALPUFF model, which is the same for the finest domain of the WRF model. The 7 locations of observation sites are indicated by diamonds.

4000 m following the given guidelines from the United States Environmental Protection Agency (US EPA)/Federal Land Manager (FLM). The Pasquille-Gifford (PG) stability calculation and the complex terrain algorithm for the partial plume path adjustment is applied. A steady-state unit emission of ^{137}Cs with the amount of 1.68 Bq s^{-1} is applied for the hypothetical radioactive leaking from the HANARO research reactor, which is slightly higher than one used for the previous study investigating the unexpected releasing incident at the Ki-Jang research reactor [3]. Stack release was set at the actual stack height of 68 m with an exit temperature of 298.15 K and an exit velocity of 32.2 m s^{-1}. The effective release height can vary depending on stack height, wind speed, atmospheric stability, and so on [14]. Dry and wet depositional processes were simulated based upon particulate characteristics. Diurnally varying deposition velocities were applied to dry depositional processes. A scavenging coefficient of 1×10^{-4} was applied for the wet deposition. Setup configuration for the other absorption characteristics of small particles is the same as the previous study by Choi et al. (2018) [3].

We used the 10-m wind from the model and observation in order to evaluate the WRF simulations. While the release height, 68 m, is higher than the wind measurement level, 10 m, both the release (68 m) and observation (10 m) heights are in the atmospheric boundary layer, where the shear- and/or buoyancy-generated turbulences mix plumes vertically throughout the boundary layer. Therefore, in terms of the plume transportation it is reasonable to expect they would show a similar temporal variability as the turbulences are the major sources of the variability in the boundary layer. The observation data for the 10-m wind was taken from the KAERI at the location of the HANARO Research Reactor, and 6 Automated Surface Observing System (ASOS) of KMA stations at Cheonan, Cheongju, Boeun, Buyeo, Geumsan, and Daejeon. The ASOS observations are available from the KMA's data portal website at http://data.kma.go.kr.

2.2. Sensitivity experiments

We set four different numerical experiments for sensitivity tests. In the control experiment, named JD, the model integrates employing the YSU PBL with the sub-grid-scale orography parameterization of Jimenez and Dudhia (JD) applied [30]. To examine the impacts followings upon the near-surface wind: (1) the sub-grid-scale orographic drag, (2) the form of stability calculation, and (3) selection among different PBL schemes; we conducted three other simulations those are named as NOJD, JD_SRDT, and NOJD_MYNN (Table 2). Comparison of the JD and the NOJD experiments examines the impact of the sub-grid-scale orographic drag. Comparison of the JD and the JD_SRDT experiments examines the influence of the stability calculation. The impact of PBL scheme selection is shown by comparing the NOJD and the NOJD_MYNN experiments. The further background information for the sensitivity experiments setup is given as follows:

- It is shown that the YSU PBL with the JD orographic drag parameterization has significantly alleviated the positive bias with respect to the wind speed at 10-m above ground, from the previous study [4]. The JD orographic drag parameterization is only available to the YSU PBL in the current WRF Model framework at this moment.
- The MMIF has two different options for calculating the PG stability class: the SRDT method [33] and the Golder method [34], which of their impacts on wind simulation are examined in this study. The SRDT method calculated the PG stability based on the 10-m wind-speed and solar radiation during the day, and the differences between the 10-m and 2-m temperatures during the night. Meanwhile, PG stability is

Table 2
Summary of the conducted experiments.

Experiment Name	PBL	Orographic Drag	Stability
JD	YSU	JD	Golder
NOJD	YSU	None	Golder
JD_SRDT	YSU	JD	SRDT
NOJD_MYNN	MYNN	None	Golder

Please cite this article as: K.-S. Sunny Lim et al., Impact of boundary layer simulation on predicting radioactive pollutant dispersion: A case study for HANARO research reactor using the WRF-MMIF-CALPUFF modeling system, Nuclear Engineering and Technology, https://doi.org/10.1016/j.net.2020.06.011

computed based on the relationships between Monin-Obukhov lengths and surface roughness in the Golder method. Previous study conducted the field tracer experiments in Daejeon and showed that the observed distribution of released tracer gas under the different weather conditions (stable or unstable) were substantially different [35]. This implies the importance of stability on the dispersion of radioactive substances.

- The MYNN PBL scheme is a 1.5-order (or turbulence kinetic energy (TKE)-order) local PBL scheme [36], whereas the YSU PBL used in other simulations is a first-order non-local PBL scheme. One of the major differences between those two schemes is in how to handle the non-local mixing. The YSU PBL considers non-local vertical mixing from the surface into any levels of the PBL driven by surface heating, which tends to improve the temperature and wind profiles during the daytime [37,38]. Among a number of PBL schemes available in the WRF model, the MYNN PBL was selected based on its structural difference with the YSU PBL (1.5-order local vs 1st-order nonlocal) [39] and its well-demonstrated good performance in both research and operational applications [39–42].

3. Results

3.1. Impact of the orographic drag

Fig. 2 shows the time-evolving root-mean-square error (RMSE) of the 10-m wind with respect to its direction and speed during the full period of the JD simulation at the seven locations shown at Fig. 1b. Note that although the instantaneous wind fields from the WRF model are used for the comparison, modeled wind fields themselves are filtered values for the temporal and spatial resolution depending on model numerical and/or physical diffusion. The RMSE values shown on each day are obtained through the comparison of hourly observed and simulated values during the 102-h of the model integration starting at 00 UTC on each day of October 2016. The averaged RMSE indicates that the JD simulation gives mean errors of 60°–100° in the wind direction and 1 m s^{-1} – 1.8 m s^{-1} in the wind speed. Relatively lower errors in wind direction are seen during two periods, which are 4–6 and 18–25 October. For wind speed, the RMSE is lower in the time period of 13–20 October than in the other period. Hence, the three simulations starting from the 18, 19, and 20 October are selected as the period of interest for examining further capabilities, since these had the smallest errors in both wind direction and wind speed.

We first compare the JD and NOJD experiments to examine the impact of the orographic drag consideration in the model. To evaluate the performance for simulating the near-surface wind during the selected periods from the 18th to 20th October, we

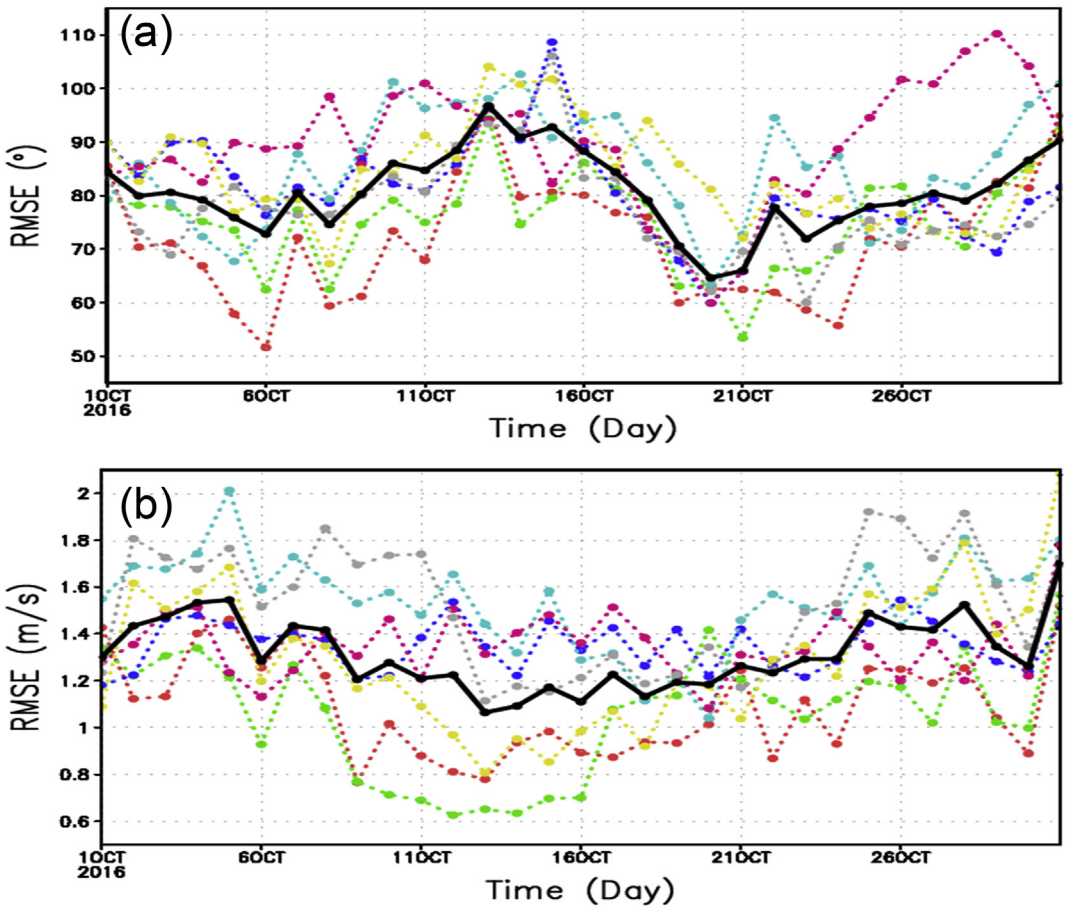

Fig. 2. The root-mean-square error (RMSE) of (a) wind direction and (b) wind speed of the JD simulation. Each colored line indicates the RMSE calculated using the wind fields observed at the 7 different observation points shown in Fig. 1b. The thick black lines indicate the averaged RMSE across observation points. Time (Day) in x-axis represents the calculation initial day.

Please cite this article as: K.-S. Sunny Lim et al., Impact of boundary layer simulation on predicting radioactive pollutant dispersion: A case study for HANARO research reactor using the WRF-MMIF-CALPUFF modeling system, Nuclear Engineering and Technology, https://doi.org/10.1016/j.net.2020.06.011

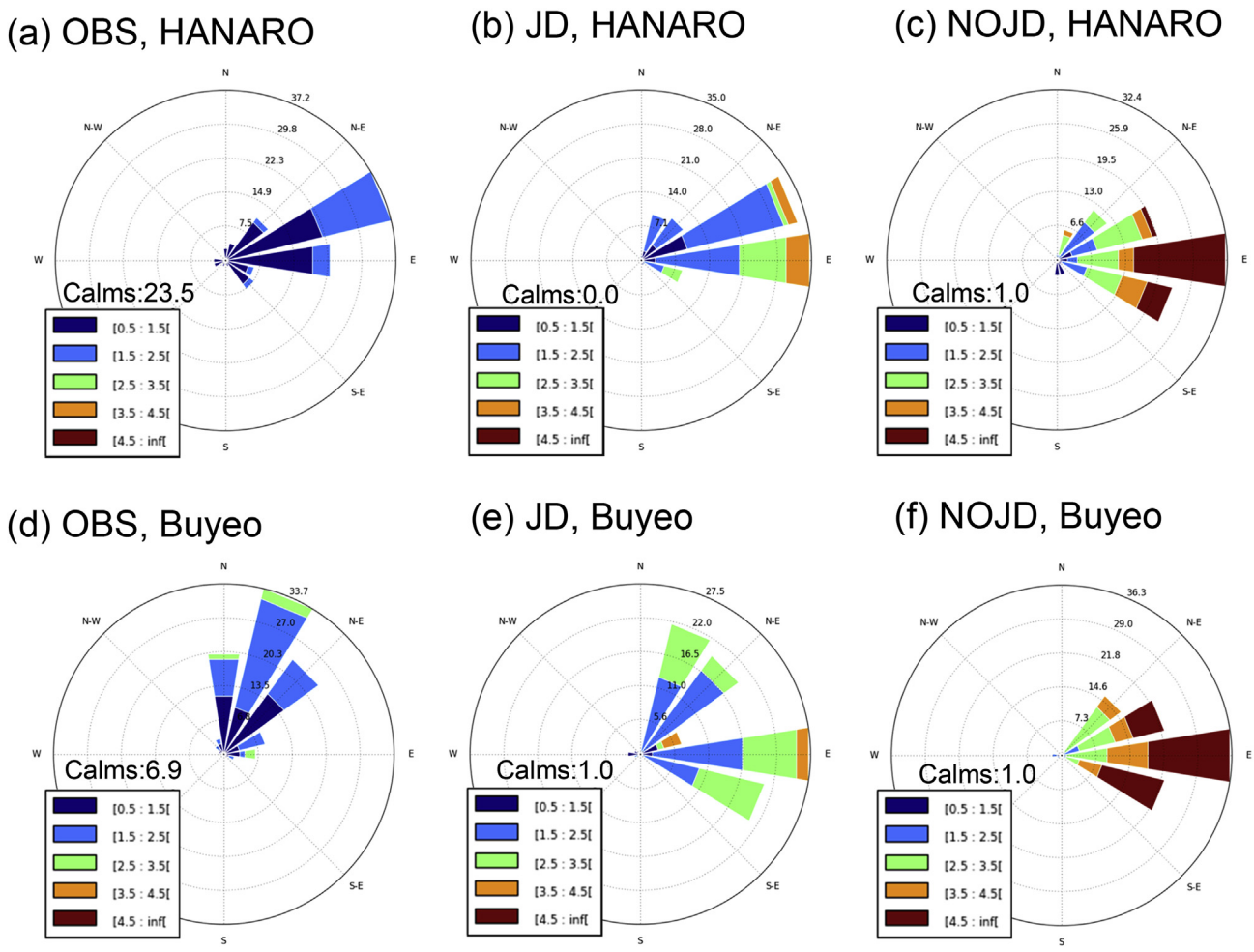

Fig. 3. Wind rose plots for 18 to 20 October 2016 at the HANARO location from (a) observation, and (b) JD and (c) NOJD simulations. (d)–(e) are the same as for (a)–(c), but at the Buyeo location. Units in [m/s].

selected two specific locations for the emission source itself (i.e., HANARO) and its wind downstream (i.e. Buyeo) (see Fig. 1b for geographical locations). Fig. 3 indicates the improvement in simulated wind for the JD experiment compared to the NOJD experiment, demonstrating that the JD experiment provided a more realistic wind simulation. The observation at HANARO (Fig. 3a) corresponded more closely to the outcome of the JD simulation (Fig. 3b) than that of the NOJD simulation (Fig. 3c). The magnitude of wind-speed overestimation is less than that in the JD simulation (Fig. 3b). The result at Buyeo shows a similar tendency, not only in terms of the wind speed but also the wind direction, whereas the JD result still gave errors in the wind direction. As noted by Lim et al. (2019) [4], implementing the JD surface drag parameterization alleviates the positive bias of wind speed in the WRF model. By considering the unresolved orography effect, a new surface sink term has been added in the conservation equation of momentum in the JD experiment, which reduces the simulated wind speed.

The simulated dispersions in the hypothetical scenario of a radioactive leak obtained from the JD and NOJD experiments are also compared to examine the influence. Fig. 4 shows the 102-h averaged dispersion factor under the hypothetical leaking scenario for both simulations, and their differences are shown in Fig. 5. For the case of 18 October, the dispersion has wider spread than those for other days. For the second case (19 October), the dispersion is stretched toward two major directions, west-northwestward and southward. For the case of 20 October, the major direction of the dispersion is westward. On 23 October, there was a light precipitation over the entire simulation domain, which can reduce Cs-137 concentration in both JD and NOJD due to wet deposition. Although the spatial patterns of dispersion were not very different for the JD and NOJD simulations (Fig. 4), the magnitude of concentration shows a noticeable difference (Fig. 5). The JD experiment simulates a larger concentration near the source point, noted as HANARO in Fig. 5, than did the NOJD simulation because of the reduced wind speed shown in Fig. 3. Han et al. (2016) used a computational fluid dynamics model to show that wind speed plays an important role in the dispersion of O_3 and NO_2 in an urban park [43]. Although it is not possible to validate the simulated concentration against observation when working with hypothetical radioactive leaking scenarios, it is reasonable to argue that the JD estimates the radioactive concentration near the reactor more conservatively.

3.2. Impact of the stability calculation

The JD and JD_SRDT experiments are compared in order to examine the stability calculated by Golder and SRDT methods and its impact upon the pollutant dispersion. The percentage of stability calculated using the two methods for the selected days are

Please cite this article as: K.-S. Sunny Lim et al., Impact of boundary layer simulation on predicting radioactive pollutant dispersion: A case study for HANARO research reactor using the WRF-MMIF-CALPUFF modeling system, Nuclear Engineering and Technology, https://doi.org/10.1016/j.net.2020.06.011

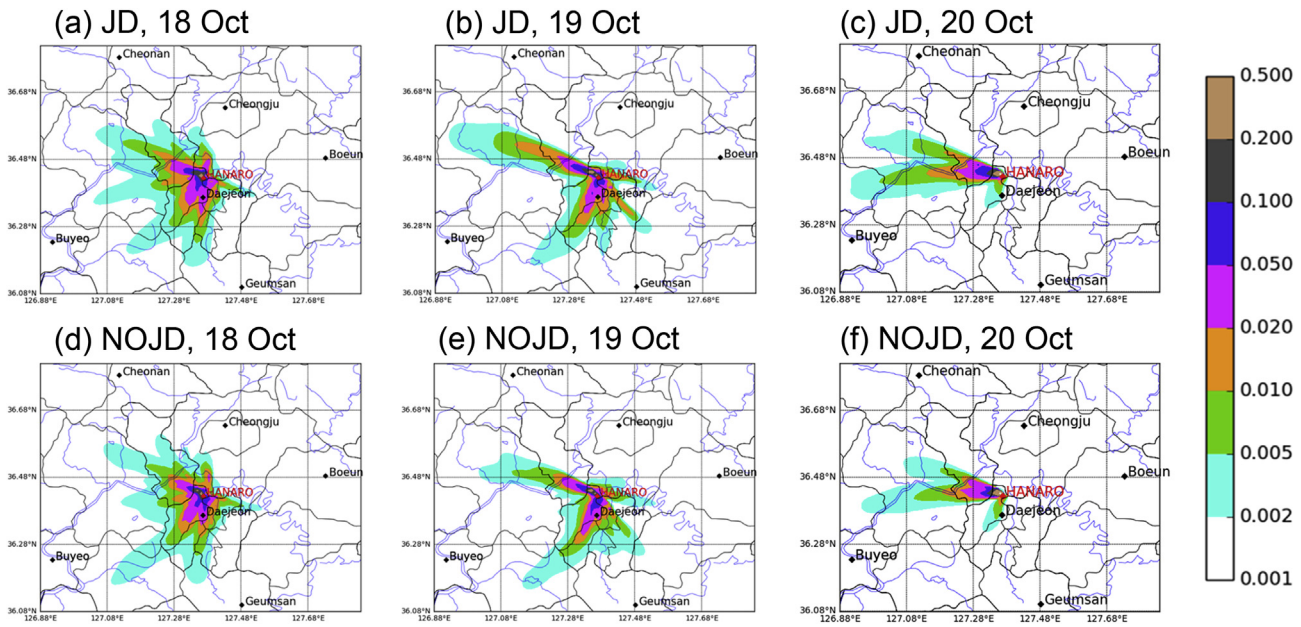

Fig. 4. The spatial distribution of 102-h-averaged dispersion factor, χ/Q (10^{-6} m^{-3} s), during the entire model integration for JD (upper column) and NOJD (lower column); (a) and (d) are results obtained from model integrations starting from 00 UTC 18 October; (b) and (d) 00 UTC 19 October; (c) and (f) 00 UTC 20 October 2016.

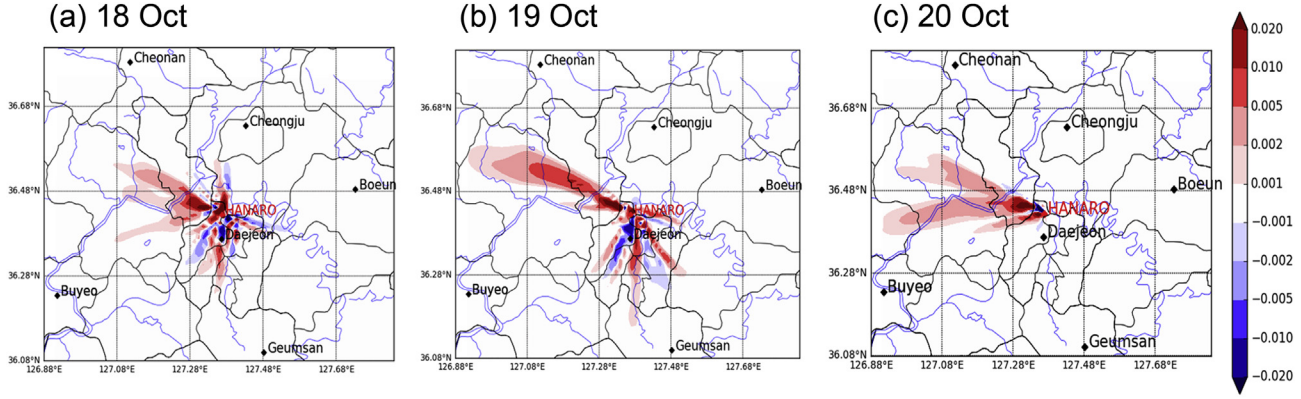

Fig. 5. The differences in the spatial distribution of 102-h-averaged dispersion factor, χ/Q (10^{-6} m^{-3} s) between JD and NOJD (JD minus NOJD). Results are obtained from model integrations starting from (a) 00 UTC 18 October, (b) 00 UTC 19 October, and (c) 00 UTC 20 October 2016.

presented in Fig. 6. For each day, the percentage is calculated from the sum of the number of grid points corresponding to each stability category divided by the total grid points. Hourly WRF output during the 102-h integration time is utilized for the calculation. The sum of the percentages from stability categories 1 to 6 is 100%. The analysis shows that the Golder method has a higher percentage for the very-stable (category 6) sides, while the SRDT gives higher percentage for the neutral stability than the other method (Fig. 6). The Golder method produces a higher percentage for the very-unstable category (category 1), compared to the SRDT method, but the difference is less than that for the very-stable category.

Fig. 7 compares the simulated dispersion prediction obtained from the JD and JD_SRDT experiments to examine the impacts of the different stability calculations. Other conditions except for the stability calculation method are set to be the same in those two different experiments, JD and JD_SRDT. Overall, the JD experiment shows larger concentration around the source than the JD_SRDT experiment because the Golder method generated more frequent stable situations than the SRDT method. This was reflected in the larger percentage of stable categories obtained from the Golder method than from the SRDT method (Fig. 6). Under the more stable environment of the Golder method, the radioactive pollutants do not disperse efficiently, which could lead to the conservative estimation of radioactive concentration around the source for when hypothetical radioactive leaking simulations.

3.3. Impact of the PBL scheme

As the PBL height is known to play an important role in modulating air quality [44], we conducted a sensitivity experiment on PBL scheme selection, by applying another PBL parameterization named MYNN (Mellor–Yamada–Nakanishi–Niino). The effect of using different PBL schemes is examined by comparing the NOJD and the NOJD_MYNN experiments, which use the YSUPBL and MYNN PBL schemes, respectively. Without sub-grid-orographic drag parameterization, the NOJD_MYNN failed to simulate the observed wind fields, showing a large positive bias (cf. Figs. 3a and 8a, and Figs. 3d and 8b). Moreover, the wind direction is biased

Please cite this article as: K.-S. Sunny Lim et al., Impact of boundary layer simulation on predicting radioactive pollutant dispersion: A case study for HANARO research reactor using the WRF-MMIF-CALPUFF modeling system, Nuclear Engineering and Technology, https://doi.org/10.1016/j.net.2020.06.011

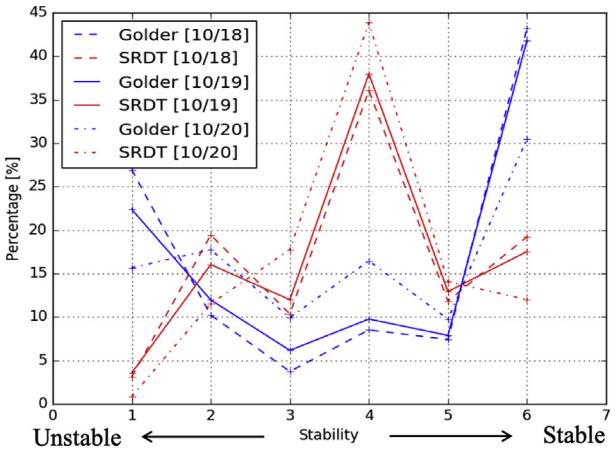

Fig. 6. The percentage of the occurance of 6 stability categories calculated using the Golder method (blue) and the SRDT method (red). A value of 1 indicates a very unstable situation, while 6 indicates a very stable situation. The dashed, dotted, and solid lines denote the percentages for different days. (For interpretation of the references to color in this figure legend, the reader is referred to the Web version of this article.)

towards the easterly relative to the observations at HANARO and Buyeo. Comparing the wind rose plots at HANARO (Figs. 3c and 8a) and Buyeo (Fig. 3f and 8b) shows the difference in the wind direction between the NOJD and the NOJD_MYNN experiments. The NOJD_MYNN experiment shows a more dominant east wind at HANARO (cf. Figs. 3c and 8a), stronger north-east to east and south-east to east winds and a weaker east wind at Buyeo (cf. Figs. 3f and 8b).

The difference in the wind direction causes the different spatial pattern of dispersion, as in Fig. 9, with less westward and more southward dispersion in the NOJD experiment compared to the NOJD_MYNN experiment on October 18th and 19th (Fig. 9a–b) due to less dominant east wind in the NOJD. The impact of the choice of PBL parameterization upon the radioactive pollutant dispersion is shown to be less significant than that of the inclusion of sub-grid-scale orography parameterization in our case, especially for the October 20th (c.f. Figs. 5c and 9c). The simulated wind fields from both NOJD and NOJD_MYNN are deviated from the observed wind fields, suggesting that the simulated dispersion characteristics of radioactive pollutants would not be very reliable without considering the orographic drag in our case.

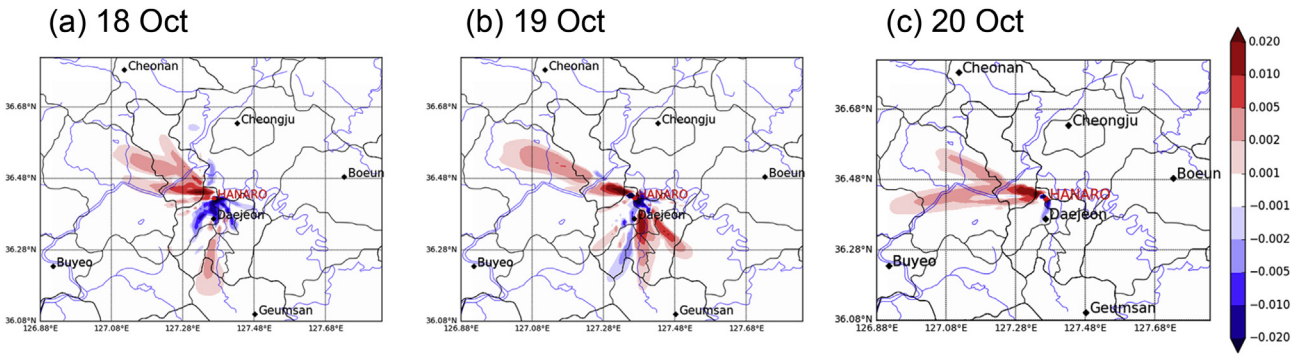

Fig. 7. The differences in the spatial distribution of 102-h-averaged dispersion factor, χ/Q (10^{-6} m^{-3} s) between JD and JD_SRDT (JD minus JD_SRDT). Results are obtained from model integrations starting from (a) 00 UTC 18 October, (b) 00 UTC 19 October, and (c) 00 UTC 20 October 2016.

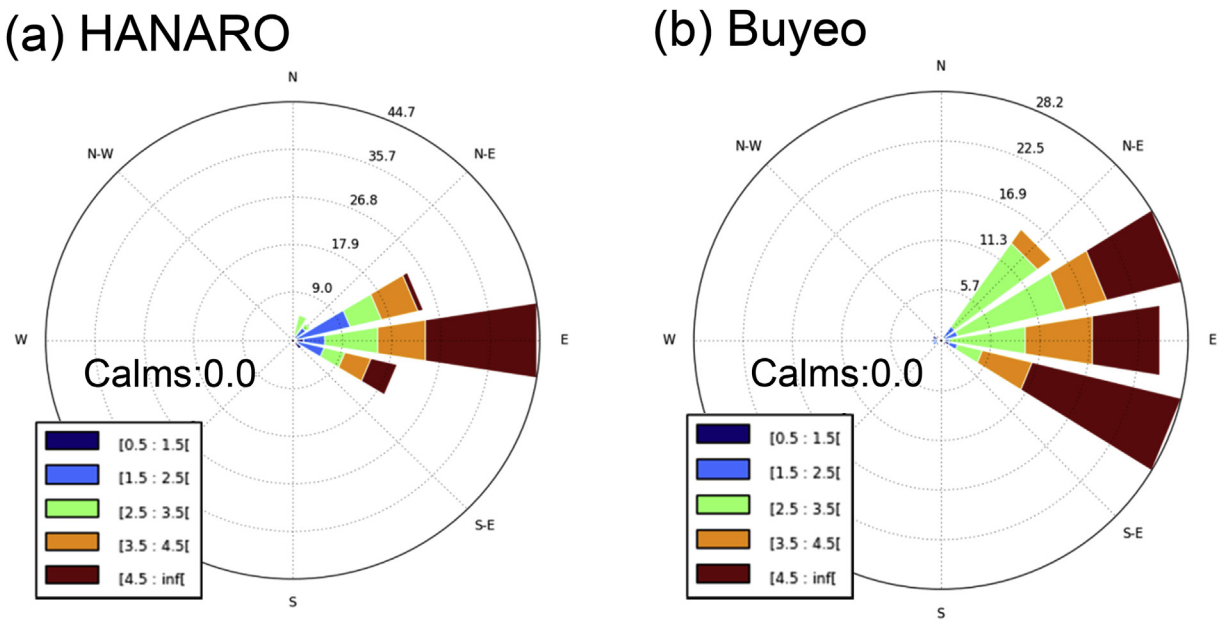

Fig. 8. Wind rose plots for 18 to 20 October 2016 obtained using the simulated wind fields from the NOJD_MYNN at the (a) HANARO and (b) Buyeo locations.

Please cite this article as: K.-S. Sunny Lim et al., Impact of boundary layer simulation on predicting radioactive pollutant dispersion: A case study for HANARO research reactor using the WRF-MMIF-CALPUFF modeling system, Nuclear Engineering and Technology, https://doi.org/10.1016/j.net.2020.06.011

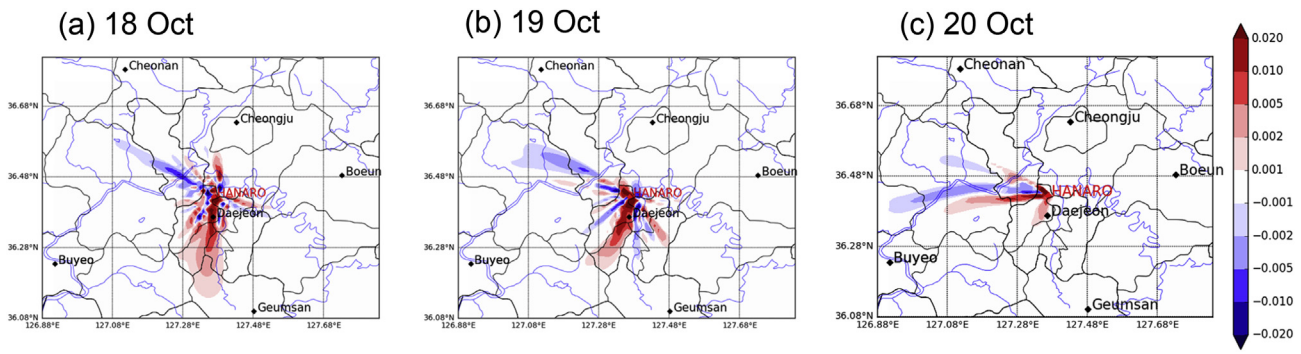

Fig. 9. The differences in the spatial distribution of 102-h-averaged dispersion factor, χ/Q (10^{-6} m^{-3} s) between NOJD_MYNN (NOJD minus NOJD_MYNN). Results are obtained from model integrations starting from (a) 00 UTC 18 October, (b) 00 UTC 19 October, and (c) 00 UTC 20 October 2016.

4. Summary and conclusions

The objective of the present study is to improve the accuracy of the radioactive dispersion prediction from the WRF-MMIF-CALPUFF modeling system by investigating the impact of the boundary layer simulation. As the wind in the lower boundary layer near the surface is one of the most important factors determining the dispersion concentration around the source [45], we focused on the 10-m wind components simulated by the system's atmospheric modeling component (i.e., WRF). The numerical simulations were conducted using the KAERI's dispersion modeling system and the influence of different methods for calculating PBL-related factors in the WRF model upon the wind prediction and corresponding dispersion of the radioactive material (^{137}Cs) was examined. In particular, the impacts of the following components related to the near-surface wind were examined: (1) orographic drag, (2) the form of stability calculation, and (3) selection among different PBL schemes.

Regarding the orographic drag, enabling the JD scheme in the YSU PBL showed the most significant improvement in the wind field by alleviating the positive bias in wind speed, thus generating less dispersion of radionuclides and a conservative dose. The different stability calculation methods also affected the dispersion concentration around the source area. The effect of the stability calculation method upon the dispersion of radioactive pollutants was significant, which is consistent to the previous study [35]. Although the application of different PBL parameterizations did not significantly improve the wind speed in the present study, the advantage of using the YSU PBL parameterization scheme (rather than the MYNN PBL scheme) in the WRF model is having the JD orographic drag as an applicable option that alleviates the overestimation of wind speed.

The results highlight the importance of considering the orographic drag in the simulation, especially over domains having complex topography, such as the Korean region. Although the nature of scenario studies is not allowing to validate the simulated dispersion concentration against the observational data that is not available, a robust improvement in the wind fields was demonstrated in our experiments. A limitation of this study is in the fact that the experiments were conducted as a case study for a single point; however, further studies for various regions using longer period experiments are enabled based on the outcomes of the present study. The information from this study is also useful for advancing the WRF-MMIF-CALPUFF dispersion modeling system in the future, to better assess the dispersion of radioactive pollutants. The simulation system established throughout this study offers the real-time forecasting capabilities for the KAERI, helping the emergency training and monitoring to be better ready for any unexpected radiative leaking incidents from nuclear reactors.

Declaration of competing interest

The authors declare that they have no known competing financial interests or personal relationships that could have appeared to influence the work reported in this paper.

Acknowledgements

The authors acknowledge the constructive and valuable comments from three anonymous reviewers. This research was supported by the Kyungpook National University Research Fund, 2018. The Lawrence Livermore National Laboratory is operated for the U. S. Department of Energy under Contract DE-AC52-07NA27344. The National Center for Atmospheric Research is sponsored by the National Science Foundation.

References

[1] G. Katata, M. Ota, H. Terada, M. Chino, H. Nagai, Atmospheric discharge and dispersion of radionuclides during the Fukushima Dai-ichi Nuclear Power Plant accident. Part I: source term estimation and local-scale atmospheric dispersion in early phase of the accident, J. Environ. Radioact. 109 (2012) 103–113.

[2] E.-C. Chang, K. Yoshimura, A semi-Lagrangian advection scheme for radioactive tracers in the NCEP Regional Spectral Model (RSM), Model Dev 8 (2015) 3247–3255, https://doi.org/10.5194/gmd-8-3247-2015.

[3] G.S. Choi, J.M. Lim, K.S.S. Lim, K.H. Kim, J.H. Lee, Characteristics of regional scale atmospheric dispersion around Ki-Jang research reactor using the Lagrangian Gaussian puff dispersion model, Nuclear Engineering and Technology 50 (1) (2018) 68–79.

[4] K.S.S. Lim, J.M. Lim, H.H. Shin, J. Hong, Y.Y. Ji, W. Lee, Impacts of sub-grid-scale orography parameterization on simulated atmospheric fields over Korea using a high-resolution atmospheric forecast model, Meteorol. Atmos. Phys. 131 (4) (2019) 975–985.

[5] W.C. Skamarock, J.B. Klemp, J. Dudhia, D.O. Gill, Z. Liu, J. Berner, W. Wang, J.G. Powers, M.G. Duda, D.M. Barker, X.-Y. Huang, A Description of the Advanced Research WRF Version 4, NCAR Tech, 2019, p. 145, https://doi.org/10.5065/1dfh-6p97. Note NCAR/TN-556+STR.

[6] U.Y. Byun, S.Y. Hong, H. Shin, J.W. Lee, J.I. Song, S.J. Hahm, J.K. Kim, H.W. Kim, J.S. Kim, WRF-based short-range forecast system of the Korea Air Force: verification of prediction skill in 2009 summer, Atmosphere 21 (2) (2011) 197–208.

[7] J.W. Lee, S.Y. Hong, A numerical simulation study of orographic effects for a heavy rainfall event over Korea using the WRF model, Atmosphere 16 (4) (2006) 319–332.

[8] S.Y. Hong, J.W. Lee, Assessment of the WRF model in reproducing a flash-flood heavy rainfall event over Korea, Atmos. Res. 93 (4) (2009) 818–831.

Please cite this article as: K.-S. Sunny Lim et al., Impact of boundary layer simulation on predicting radioactive pollutant dispersion: A case study for HANARO research reactor using the WRF-MMIF-CALPUFF modeling system, Nuclear Engineering and Technology, https://doi.org/10.1016/j.net.2020.06.011

[9] H.H. Park, J. Lee, E.C. Chang, M. Joh, High-resolution simulation of snowfall over the Korean eastern coastal region using WRF model: sensitivity to domain nesting-down strategy, Asia-Pacific Journal of Atmospheric Sciences (2019) 1–14.
[10] S.Y. Hong, N.K. Moon, K.S.S. Lim, J.W. Kim, Future climate change scenarios over Korea using a multi-nested downscaling system: a pilot study, Asia-Pacific Journal of Atmospheric Sciences 46 (4) (2010) 425–435.
[11] E.S. Im, J.B. Ahn, S.R. Jo, Regional climate projection over South Korea simulated by the HadGEM2-AO and WRF model chain under RCP emission scenarios, Clim. Res. 63 (3) (2015) 249–266.
[12] J. Lee, H.H. Shin, S.-Y. Hong, P.A. Jiménez, J. Dudhia, J. Hong, Impacts of subgrid-scale orography parameterization on simulated surface layer wind and monsoonal precipitation in the high-resolution WRF model, J. Geophys. Res. 120 (2) (2015) 644–653.
[13] D. Lee, S.K. Min, J. Jin, J.W. Lee, D.H. Cha, M.S. Suh, J.B. Ahn, S.Y. Hong, H.S. Kang, M. Joh, Thermodynamic and dynamic contributions to future changes in summer precipitation over Northeast Asia and Korea: a multi-RCM study, Clim. Dynam. 49 (11–12) (2017) 4121–4139.
[14] J.S. Scire, D.G. Strimaitis, R.J. Yamartino, A User's Guide for the CALPUFF Dispersion Model, Earth Tech, Inc., Concord, MA, 2000, p. 10.
[15] United States Environmental Protection Agency (EPA), Analyses of the CALMET/CALPUFF Modeling System in a Screening Mode, Office of Air Quality Planning and Standards, Research Triangle Park, NC, 1998. EPA-454/R-98-010.
[16] S.Y. Hong, Y. Noh, J. Dudhia, A new vertical diffusion package with an explicit treatment of entrainment processes, Mon. Weather Rev. 134 (9) (2006) 2318–2341.
[17] S.Y. Hong, A new stable boundary-layer mixing scheme and its impact on the simulated East Asian summer monsoon, Q. J. R. Meteorol. Soc. 136 (651) (2010) 1481–1496.
[18] Y. Noh, W.G. Cheon, S.Y. Hong, S. Raasch, Improvement of the K-profile model for the planetary boundary layer based on large eddy simulation data, Boundary-Layer Meteorol. 107 (2) (2003) 401–427.
[19] D.-H. Cha, D.-K. Lee, S.-Y. Hong, Impacts of boundary layer processes on seasonal simulation of the East Asia summer monsoon using a Regional Climate Model, Meteorol. Atmos. Phys. 100 (2009) 53–72.
[20] K.-S.S. Lim, S.-Y. Hong, J.-H. Yoon, J. Han, Simulation of the summer monsoon rainfall over East Asia using the NCEP GFS cumulus parameterization at different horizontal resolutions, Weather Forecast. 29 (2014) 1143–1154.
[21] K.-S.S. Lim, S.-Y. Hong, Investigation of aerosol indirect effects on simulated flash-flood heavy rainfall over Korea, Meteorol. Atmos. Phys. 118 (2012) 199–214.
[22] W.C. Skamarock, J.B. Klemp, J. Dudhia, D.O. Gill, D.M. Barker, M.G. Duda, X.-Y. Huang, W. Wang, J.G. Powers, A Description of the Advanced Research WRF Version 3, NCAR Tech, 2008, p. 113, https://doi.org/10.5065/D68S4MVH. Note NCAR/TN-475+STR.
[23] S.Y. Hong, J.O.J. Lim, The WRF single-moment 6-class microphysics scheme (WSM6), Asia-Pacific Journal of Atmospheric Sciences 42 (2) (2006) 129–151.
[24] J. Dudhia, S.Y. Hong, K.S. Lim, A new method for representing mixed-phase particle fall speeds in bulk microphysics parameterizations, Journal of the Meteorological Society of Japan. Ser. II 86 (2008) 33–44.
[25] J.S. Kain, The Kain–Fritsch convective parameterization: an update, J. Appl. Meteorol. 43 (1) (2004) 170–181.
[26] J.S. Kain, J.M. Fritsch, A one-dimensional entraining/detraining plume model and its application in convective parameterization, J. Atmos. Sci. 47 (23) (1990) 2784–2802.
[27] F. Chen, J. Dudhia, Coupling an advanced land surface–hydrology model with the Penn State–NCAR MM5 modeling system. Part I: model implementation and sensitivity, Mon. Weather Rev. 129 (4) (2001) 569–585.
[28] M.J. Iacono, J.S. Delamere, E.J. Mlawer, M.W. Shephard, S.A. Clough, W.D. Collins, Radiative forcing by long-lived greenhouse gases: calculations with the AER radiative transfer models, J. Geophys. Res.: Atmosphere 113 (D13) (2008).
[29] J.-J. Morcrette, H.W. Barker, J.N.S. Cole, M.J. Iacono, R. Pincus, Impact of a new radiation package, McRad, in the ECMWF integrated forecasting system, Mon. Weather Rev. 136 (2008) 4773–4798, https://doi.org/10.1175/2008MWR2363.1.
[30] P.A. Jimenez, J. Dudhia, Improving the representation of resolved and unresolved topographic effects on surface wind in the WRF model, Journal of Applied Meteorology and Climatology 51 (2012) 300–316.
[31] M. Werner, Shuttle radar topography mission (SRTM), mission overview, Jpn. Telecom. 55 (2001) 75–79.
[32] B. Rabus, M. Eineder, R. Am, R. Bamler, The shuttle radar topog- raphy mission—a new class of digital elevation models acquired by space borne radar, J Photogramm Remote Sens 57 (2004) 241–262.
[33] EPA, "An evaluation of a solar radiation/delta-T (SRDT) method for estimating pasquill-gifford (P–G) stability categories, in: Technical Report Prepared by the U.S. Environmental Protection Agency, Office of Air Quality Planning and Standards, 1993. Research Triangle Park, NC (EPA–454/R–93–055).
[34] D. Golder, Relations among stability parameters in the surface layer, Boundary-Layer Meteorol. 3 (1972) 47–58.
[35] M.H. Han, E.H. Kim, H.J. Jeong, H.S. Jeong, M.S. Park, W.T. Hwang, Field tracer experiments under severe weather conditions for the validation of the dispersion of radioactive materials, Journal of Radiation Protection 38 (4) (2013) 208–2013.
[36] M. Nakanishi, H. Niino, Development of an improved turbulence closure model for the atmospheric boundary layer, J. Meteorol. Soc. Jpn. 87 (2009) 895–912.
[37] A.A.M. Holtslag, B.A. Boville, Local versus nonlocal boundary-layer diffusion in a global climate model, J. Clim. 6 (1993), 1925-1842.
[38] H.H. Shin, S.-Y. Hong, Inter-comparison of planetary boundary-layer parametrizations in the WRF model for a single day from CASES-99, Boundary-Layer Meteorol. 139 (2) (2011) 261–281.
[39] B. Yang, L.K. Berg, Y. Qian, C. Wang, Z. Hou, Y. Liu, H.H. Shin, S. Hong, M. Pekour, Parametric and structural sensitivities of turbine-height wind speeds in the boundary layer parameterizations in the Weather Research and Forecasting model, J. Geophys. Res.: Atmosphere 124 (2019) 5951–5969.
[40] D. Munõz-Esparza, B. Canñadillas, T. Neumann, J. van Beeck, Turbulent fluxes, stability and shear in the offshore environment: mesoscale modeling and field observations at FINO1, J. Renew. Sustain. Energy 4 (2012), 063236.
[41] S.G. Benjamin, Co-authors, A north American hourly assimilation and model forecast cycle: the Rapid refresh, Mon. Weather Rev. 144 (2016) 1669–1694.
[42] D.E.K. Dzebre, M.S. Adaramola, A preliminary sensitivity study of planetary boundary layer parameterization schemes in the Weather Research and Forecasting model to surface winds to coastal Ghana, Renew. Energy 146 (2020) 66–86.
[43] B.-S. Han, K.-H. Kwak, J.-J. Baik, Diurnal variations of O3 and NO2 concentrations in an urban park in summer: effects of air temperature and wind speed, Journal of Korean Society for Atmospheric Environment 32 (2016) 536–546.
[44] Y.-H. Ryu, J.-J. Baik, K.-H. Kwak, S. Kim, N. Moon, Impacts of urban land-surface forcing on ozone air quality in the Seoul metropolitan area, Atmos. Chem. Phys. 13 (2013) 2177–2194.
[45] J.C. Chang, P. Franzese, K. Chayantrakom, S.R. Hanna, Evaluations of CALPUFF, HPAC, and VLSTRACK with two mesoscale field datasets, J. Appl. Meteorol. 42 (2003) 453–466.

Please cite this article as: K.-S. Sunny Lim et al., Impact of boundary layer simulation on predicting radioactive pollutant dispersion: A case study for HANARO research reactor using the WRF-MMIF-CALPUFF modeling system, Nuclear Engineering and Technology, https://doi.org/10.1016/j.net.2020.06.011